

Supplementary Information

Anchoring-Group-Controlled Self-Assembly and Charge Transport in Antiaromatic Molecular Systems

Shintaro Fujii,^{*a} Koshiro Isono,^b Kazuki Nabeyama,^a Ji-Young Shin,^b Hiroshi Shinokubo,^{*b} and Tomoaki Nishino^{*a}

^a *Department of Chemistry, School of Science, Institute of Science Tokyo, 2-12-1 W4-10 Ookayama, Meguro-ku, Tokyo 152-8551, Japan*

^b *Department of Applied Chemistry, Graduate School of Engineering, Nagoya University, Aichi, 464-8603, Japan*

Table of contents

1. Synthesis of compounds 2 and 3
2. STM imaging
3. Single-molecule conductance measurements and data analysis

Supplementary Information 1. Synthesis of compounds 2 and 3

Preparation of 1,9-dibromo-5-(4-*tert*-butoxycarbonylphenyl)dipyrrin Ni(II) complex (S1)

To a 200 mL round-bottom flask, 4-*tert*-butoxycarbonylphenyl-2,2'-dipyrrromethane (2.00 g, 6.20 mmol) was evacuated and then refilled with N₂. To the flask, dry THF (120 mL) was added. The solution was cooled to -78 °C. *N*-bromosuccinimide (2.20 g, 12.4 mmol) was added to the solution in three portions with an interval of 10 min. The mixture was stirred for 1 h. To the mixture, 2,3-dichloro-5,6-dicyano-1,4-benzoquinone (DDQ, 1.54 g, 6.81 mmol) was added. The mixture was stirred at -78 °C for 30 min and at room temperature for 1 h. The reaction mixture was passed through an alumina pad and evaporated under reduced pressure. To a 200 mL flask containing the residual solid, CH₂Cl₂ (75 mL), MeOH (25 mL), and Ni(OAc)₂·4H₂O (768 mg, 3.09 mmol) were added. After stirring at room temperature for 1 h, the mixture was evaporated under reduced pressure. The residue was passed through an alumina pad with CH₂Cl₂. The solvent was removed under reduced pressure to afford 1,9-dibromo-5-(4-*tert*-butoxycarbonylphenyl)dipyrrin Ni(II) complex **S1** in 85% yield (2.65 g, 2.61 mmol) as a green solid. The ¹H and ¹³C NMR spectra of **S1** could not be observed owing to its paramagnetic nature.

Preparation of Ni(II) di(4-*tert*-butoxycarbonylphenyl)norcorrole (S2)

To a 500 mL round-bottom flask, **S1** (500 mg, 0.49 mmol) and 2,2'-bipyridyl (308 mg, 1.97 mmol) were added. In an argon-filled glovebox, Ni(cod)₂ (541 mg, 1.97 mmol) and THF (250 mL) were added to the flask. The solution was stirred for 4 h at room temperature. The reaction was quenched with chloranil (120 mg, 0.49 mmol). After filtration of the mixture through Celite, the mixture was evaporated under reduced pressure. The mixture was passed through a short silica gel column chromatography using CH₂Cl₂ and evaporated under reduced pressure. The residue was purified by silica gel column chromatography with a hexane/CH₂Cl₂ (v/v = 1/1) mixture to afford **S2** in 53% yield (180 mg, 0.27 mmol) as a black solid.

¹H NMR (500 MHz, CDCl₃, 298 K): δ = 7.43 (d, *J* = 8.5 Hz, 4H, Ar-H), 6.52 (d, *J* = 8.4 Hz, 4H, Ar-H), 3.49 (d, *J* = 4.1 Hz, β-H), 3.11 (d, *J* = 4.2 Hz, β-H), 1.43 (s, 18H, *t*-Bu) ppm; ¹³C NMR (126 MHz, CDCl₃, 298 K): δ = 164.4, 163.1, 151.4, 144.8, 137.2, 134.1, 130.3, 128.8, 123.8, 116.8, 81.2, 28.0 ppm. HRMS (APCI-TOF): [M+H]⁺ Calcd for C₄₀H₃₄N₄NiO₄ 693.2006; Found 693.1999.

Preparation of Ni(II) di(4-carboxyphenyl)norcorrole (2)

To a 30 mL round-bottom flask containing **S2** (140 mg, 0.20 mmol), concentrated H₂SO₄ (3 mL) was added, and the solution was stirred for 10 min at 0 °C. The mixture was then diluted with cold water, and the resulting solid was filtered. Then the solid was washed with cold water and acetone to afford Ni(II) norcorrole **2** in 79% yield (92 mg, 0.16 mmol) as a black solid. ¹H NMR (500 MHz, DMF-*d*₇, 298 K): δ =

7.53 (d, $J = 8.1$ Hz, 4H, Ar-H), 6.57 (d, $J = 7.4$ Hz 4H, Ar-H), 3.27 (brs, 4H, β -H), 3.00 (brs, 4H, β -H) ppm. The COOH proton was not observed. Due to its low solubility, the ^{13}C NMR spectrum of **2** could not be obtained. HRMS (MALDI-TOF): $[\text{M}]^+$ Calcd for $\text{C}_{32}\text{H}_{18}\text{N}_4\text{NiO}_4$ 580.0676; Found 580.0675.

Preparation of 1,9-dibromo-5-(4-pyridyl)dipyrin Ni(II) complex (**S3**)

To a 200 mL round-bottom flask, 4-pyridyl-2,2'-dipyrromethane (2.00 g, 8.96 mmol) was evacuated and then refilled with N_2 . To the flask, dry THF (120 mL) was added. After the solution was cooled to -78 °C, *N*-bromosuccinimide (3.19 g, 17.9 mmol) was added to the solution in three portions with an interval of 5 min. The mixture was stirred for 45 min. To the mixture, 2,3-dichloro-5,6-dicyano-1,4-benzoquinone (DDQ, 1.54 g, 6.80 mmol) was added. The mixture was stirred at -78 °C for 30 min and at room temperature for 1 h. The reaction mixture was passed through an alumina pad and evaporated under reduced pressure. To a 300 mL flask containing the residual solid, CH_2Cl_2 (140 mL), MeOH (70 mL), $\text{Ni}(\text{OAc})_2 \cdot 4\text{H}_2\text{O}$ (656 mg, 2.64 mmol) were added. After stirring at room temperature for 1 h, the mixture was evaporated under reduced pressure. The residue was passed through an alumina pad using CH_2Cl_2 and a $\text{CH}_2\text{Cl}_2/\text{MeOH}$ mixture. The solvent was removed under reduced pressure to afford **S3** in 55% yield (1.91 g, 2.34 mmol) as a green solid. The ^1H and ^{13}C NMR spectra of **S3** could not be observed owing to its paramagnetic nature.

Preparation of Ni(II) di(4-pyridyl)norcorrole (**3**)

To a 500 mL round-bottom flask, **S3** (450 mg, 0.54 mmol) and 2,2'-bipyridyl (337 mg, 2.16 mmol) were added. $\text{Ni}(\text{cod})_2$ (594 mg, 2.16 mmol) and THF (180 mL) were added to the flask in an argon-filled glovebox. The solution was stirred for 4 h at room temperature. The reaction was quenched with chloranil (132 mg, 0.54 mmol). The reaction mixture was evaporated under reduced pressure. Then, HCl aq. (1 M) was added to the residue, and the mixture was neutralized with aqueous NaHCO_3 . The mixture was then filtered. The residue was purified by silica gel column chromatography using a $\text{CH}_2\text{Cl}_2/\text{MeOH}$ ($v/v = 100/1$) mixture to afford **3** in 15% yield (41 mg, 0.08 mmol) as a black solid. ^1H NMR (500 MHz, CDCl_3 , 298 K): $\delta = 8.18$ (d, 4H, $J = 4.0$ Hz, Ar-H), 6.39 (d, 4H, $J = 4.5$ Hz, Ar-H), 3.57 (d, 4H, $J = 3.5$ Hz, β -H), 3.20 (d, 4H, $J = 3.5$ Hz, β -H) ppm. Due to its low solubility, the ^{13}C NMR spectrum of **3** could not be obtained. HRMS (APCI-TOF): $[\text{M}+\text{H}]^+$ Calcd for $\text{C}_{28}\text{H}_{16}\text{N}_6\text{Ni}$ 495.0863; Found 495.0844.

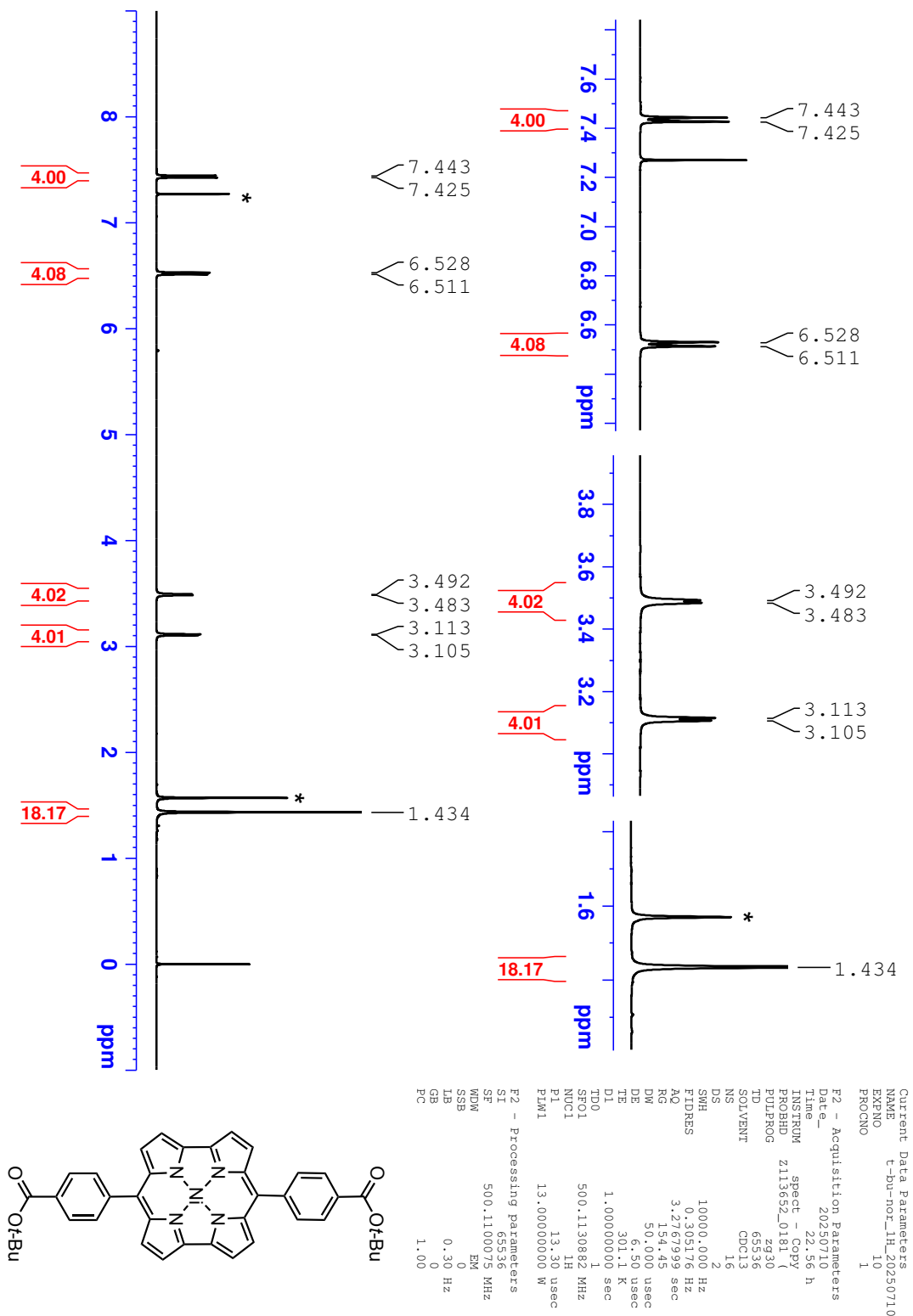
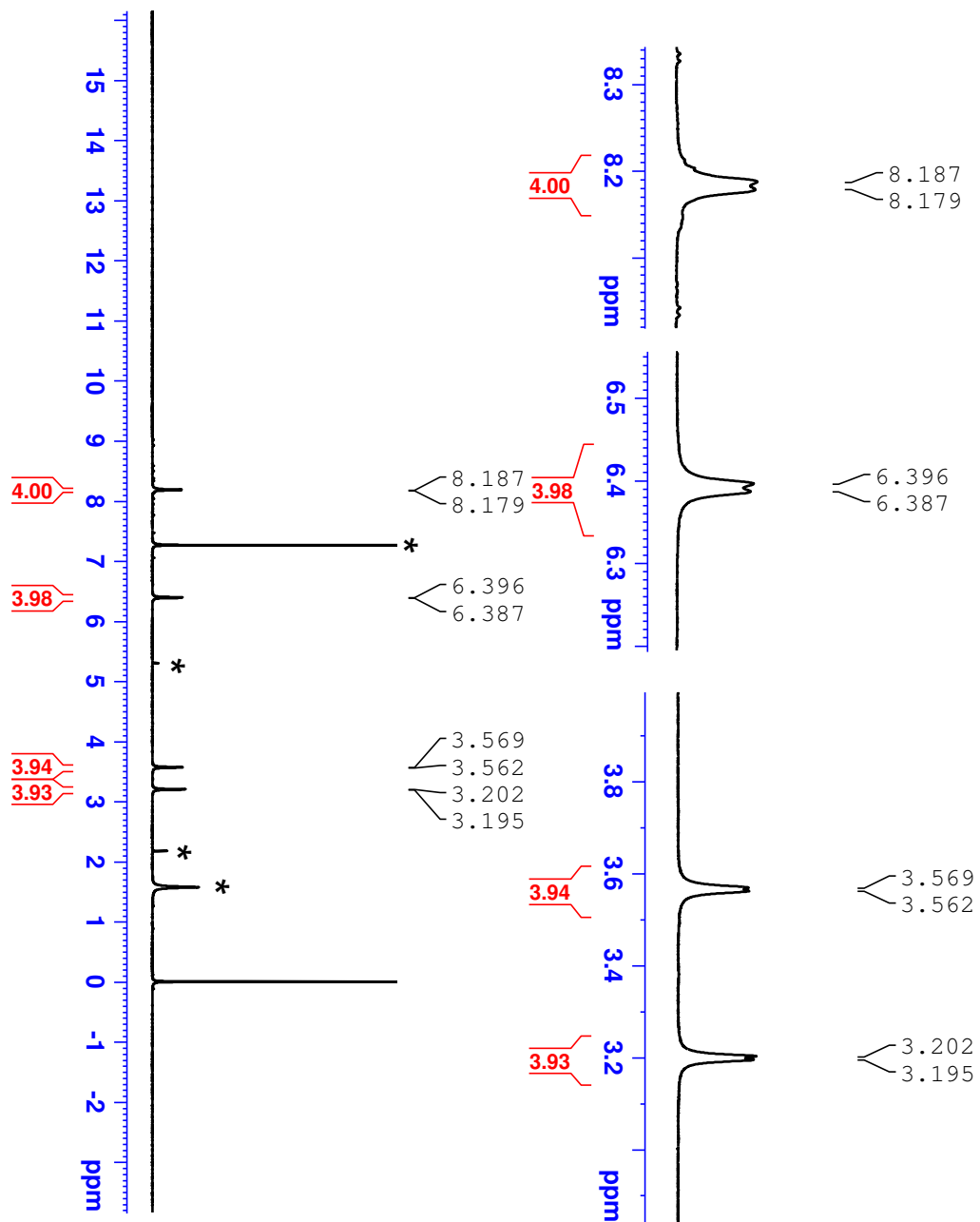


Fig. S1 ¹H NMR (500 MHz) spectrum of S2 in CDCl₃ at 25 °C (*solvent peaks).



```

Current Data Parameters
NAME      r353_Py-moC_pur13_20231129
EXPNO     10
PROCNO    1
F2 - Acquisition Parameters
Date_     20231129
Time      11:51:03
INSTRUM   spect
PROBHD    211970L_0128 (
PULPROG   zgpg30
TD         65536
SOLVENT   CDCl3
NS         16
DS         4
SWH        10000.000 Hz
FIDRES     0.1205176 Hz
AQ         3.44
RG         190.44
DM         50.000 usec
DE         291.4
TE         1.00000000 sec
D1         1.00000000 sec
SFO1      500.6530873 MHz
NUC1       1H
P1         11.75 usec
FWHM      25.7940059 Hz
F2 - Processing parameters
SI         32768
WFWD      500.0500104 MHz
GB         0
PC         1.00
  
```

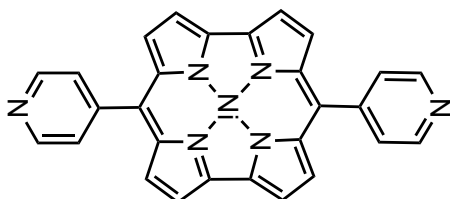


Fig. S3 ¹H NMR (500 MHz) spectrum of **3** in CDCl₃ at 25 °C (*solvent peaks).

Supplementary Information 2. STM imaging

Fig. S4 shows a constant-current STM image of the self-assembled monolayer (SAM) of **1** on Au(111), together with a cross-sectional profile taken along a molecular lattice in the STM image. The intermolecular spacing exceeds the typical value of ~ 0.5 nm observed for closely packed alkanethiol SAMs on Au(111) adopting the $\sqrt{3} \times \sqrt{3}R30^\circ$ adsorption structure.^{S1,S2} The cross-sectional profile indicates dense molecular packing without apparent voids, consistent with thiol-based SAMs on Au(111).

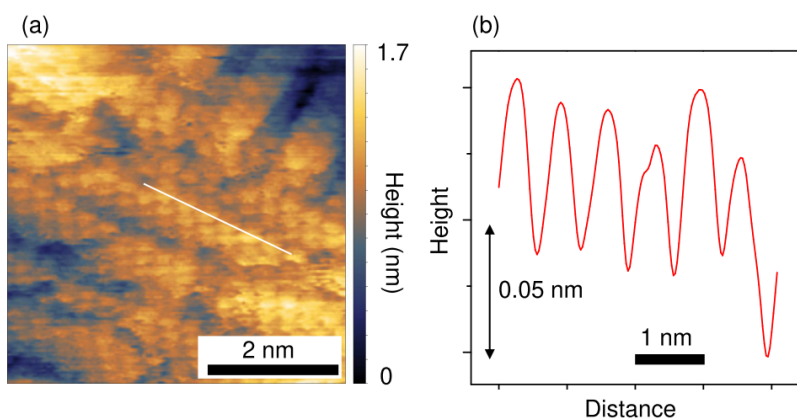


Fig. S4 (a) STM image of thiol-anchored Ni(nor) (**1**) on Au(111) (Sample bias voltage (V_s) = 1.0 V, tunnelling current (I_t) = 0.1 nA). (b) A cross-sectional profile of a molecular row along a white line in (a).

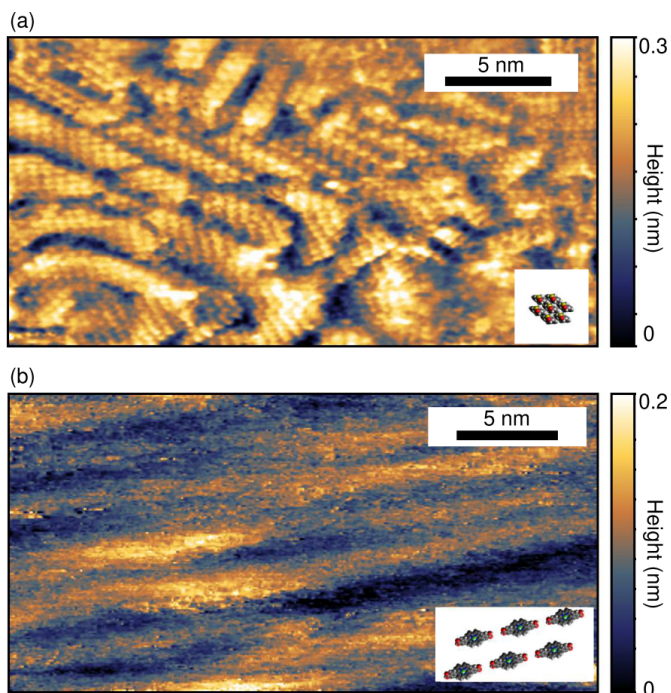


Fig. S5 STM images of (a) thiol-anchored Ni(nor) (**1**) and (b) carboxylic acid-anchored Ni(nor) (**2**) on Au(111) shown at comparable spatial scales. Imaging conditions are similar to those used in Fig. 2. Insets show schematic illustrations of the proposed adsorption geometries using space-filling models, scaled for qualitative comparison with the STM images.

Fig. S6 shows a constant-current STM image of a molecular film of **3** on Au(111). Compound **3** does not exhibit well-ordered surface assemblies; instead, its adsorption is predominantly disordered. Each bright spot in Fig. S5b is several nanometers in size, corresponding to the lateral dimension of compound **3** (approximately 2 nm).

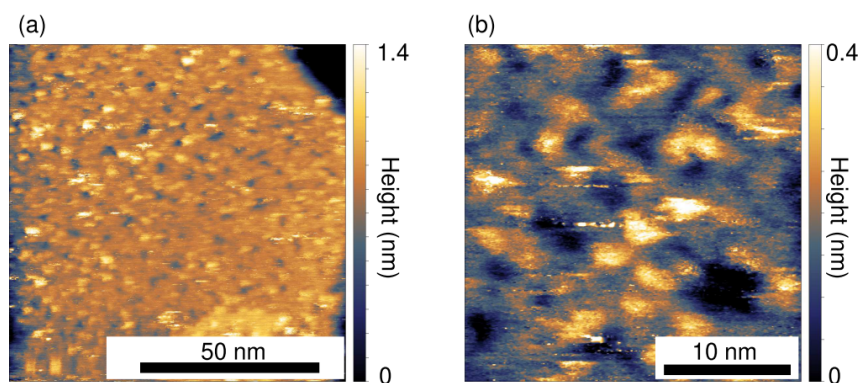


Fig. S6 (a) STM image of pyridine-anchored Ni(nor) (**3**) on Au(111) ($V_s = 1.0$ V, $I_t = 0.2$ nA). (b) STM image acquired under $V_s = 0.8$ V and $I_t = 0.3$ nA

Supplementary Information 3. Single-molecule conductance measurements and data analysis

Single-molecule conductance measurements were performed using the STM break-junction (STM-BJ) technique at room temperature, as described in the main text. Conductance–distance traces were recorded at bias voltages of 0.1–0.3 V under both ultra-high vacuum (UHV) and ambient conditions using a LabVIEW-based data acquisition system. At higher bias voltages (0.3 V), the apparent conductance resolution in the two-dimensional conductance–distance histograms becomes coarser compared to measurements performed at lower bias (0.1 V). This effect does not reflect an intrinsic change in the charge-transport mechanism of the molecular junctions. Instead, it arises from the experimental acquisition settings required to ensure stable measurements and an adequate signal-to-noise ratio at higher bias. Specifically, the current range and corresponding analogue-to-digital conversion settings were adjusted to accommodate the increased current levels, which leads to a reduced effective current resolution and results in discretised conductance levels when plotted on a logarithmic scale. Importantly, the conductance bin size used for constructing all one- and two-dimensional histograms was kept identical for all datasets [$\Delta\log(G/G_0) = 0.01$]. The observed difference in visual conductance resolution therefore originates from the measurement electronics and data acquisition parameters, rather than from any physical change in molecular junction behavior.

References

[S1] F. Schreiber, *Prog. Surf. Sci.*, 2000, **65**, 151–257.

[S2] G. E. Poirier, *Chem. Rev.*, 1997, **97**, 1117–1127.